Do we need complex mechanistic photoacclimation models for phytoplankton?

Kevin J. Flynn

Ecology Research Unit, Wallace Building, University of Wales-Swansea, Swansea SA2 8PP, Wales, United Kingdom

Abstract

The outputs of simple models relating phytoplankton growth and chlorophyll *a* (Chl *a*) to irradiance and nutrient (nitrogen [N] and/or iron [Fe]) availability are compared with those of complex mechanistic models. Mechanistic models, which are significantly more expensive in computational terms, are required for a proper description of high-resolution dynamics of light acclimation with or without changes in nutrient status (for example, with diurnal light–dark periodicity or Fe fertilization). However, for instances in which such detailed descriptions of growth and Chl:carbon (C) are not required, there appears to be no justification for using mechanistic models to simulate nutrient–light interaction. Multinutrient models based on modified quota–type models, coupled with a simple photosynthesis–irradiance growth rate equation and an empirically derived Chl *a*:C relationship linking irradiance to growth rate, should be adequate for most oceanographic modeling scenarios.

Mathematic models of phytoplankton have various applications, but invariably, a commonly required output is growth rate as a function of irradiance and nutrient availability, while a common input of real data is chlorophyll *a* (Chl *a*). It is necessary, then, to relate Chl *a* to algal biomass as carbon (C) or nitrogen (N) and, hence, with changes over time, to biomass growth. However, a major potential problem is that the relationship between Chl *a* and biomass is not constant but may vary over fivefold to 10-fold with growth irradiance and nutritional status. This range is of similar magnitude to the biomass changes (often expressed in terms of Chl *a*) documented during blooms. Accounting adequately for changes in Chl:biomass in models is thus important.

Other than accepting a fixed ratio of Chl:biomass within simulations, which is to be avoided (Marañón and Holligan 1999), there are two basic approaches to the problem. One is to use a 'forward' calculation method, constructing a mechanistic model that responds to changes in irradiance (E) and nutrient availability. The response uses feedback processes akin to those in real organisms (balancing demands for C, energy, and other nutrients), and, hence, there is a temporal element to the acclimation process that is important to reproduce for detailed simulations (Flynn et al. 2001). In such models, algal Chl content is a state variable, a 'quota,' typically as Chl:C (Doney et al. 1996; Flynn and Flynn 1998; Geider et al. 1998) or Chl:cell (Zonneveld 1998). Growth rate is then a function of the Chl quota, making reference to a Chl-specific initial slope (α^{Chl}) for the photosynthesis–irradiance (PE) curve.

The alternative approach is to use a 'reverse' method, in which some form of empirical relationship is used between irradiance and nutrient availability to derive Chl:biomass (Cloern et al. 1995; Behrenfeld et al. 2002). Here growth makes reference to a biomass-specific PE slope constant, α^B (e.g., C-specific; α^C). This reverse method has the attraction that it is less demanding of processing power, lacking a Chl: biomass state variable and equally, if not more important, the need for a small integration step size to support its calculation.

There is another type of reverse methodology, which computes Chl:C by optimization through the solution of simultaneous equations, deriving Chl:C by balancing light and nutrient limitations at each time point (Laws and Bannister 1980; Kiefer and Mitchell 1983; Laws and Chalup 1990; Hurtt and Armstrong 1996). This approach also gives instantaneous changes in Chl:C (rather than describing the temporal acclimation simulated by forward methods), but has the computational complication of solving simultaneous equations.

Balancing simplicity and realism of output is a basic tenant in modeling. Although there is no such thing as a perfect or ideal model, certainly there are such things as bad or dysfunctional models (with respect to models of phytoplankton, *see* Flynn 2003). Defining what constitutes dysfunctional behavior is not always easy, especially when, as here, there are surprisingly few data sets for ecologically important species and even fewer from studies conducted under a wide range of conditions of light- and nutrient-limited growth. Here I consider whether it is possible to obtain growth-E and Chl:C outputs from models employing the reverse methodology matching those using dynamic mechanistic forward methods. This assumes that the latter are themselves realistic (not dysfunctional) in output, but there is evidence that such models, when properly tuned, do fulfill that requirement (Geider et al. 1998; Flynn et al. 2001). The nutrients that are considered here are N and iron (Fe), as these impact on the PE curve and Chl:C in different ways, as described below.

The simulations were run through into steady state for comparison. In support of this action, it should be noted that the basis of most phytoplankton models in oceanographic simulations is Monod or quota; these models were developed and are only really applicable under steady-state conditions, even though they are widely used in dynamic simulations (Flynn 2003). While two wrongs do not make a right, it is argued that in the first instance, and for applications in which simulations are run over months and years (while photoacclimation takes place in hours and days), it is important to

Table 1. Description of parameters. Substitute C, N or Fe for X, as required.

Parameter	Units	Description
α^{Chl}	gC g^{-1} Chl μmol^{-1} photon m^{-2}	Chlorophyll-specific initial slope of growth-irradiance curve
α^X	gX g^{-1}X μmol^{-1} photon m^{-2}	X-specific initial slope of growth-irradiance curve
ChlC	gChl g^{-1}C	Chlorophyll:C mass ratio
ChlC$_{min}$	gChl g^{-1}C	Minimum value of ChlC
E	μmol photon m^{-2} s^{-1}	Irradiance
FeCo$_{min}$	gFe g^{-1}C	Minimum value of FeC$_{min}$ (see Eq. 6 and adjoining text)
FeCo$_{max}$	gFe g^{-1}C	Minimum value of FeC$_{max}$ (see Eq. 6 and adjoining text)
K$_E$	μmol photon m^{-2} s^{-1}	Constant for calculation of FeC$_{min}$ (see Eq. 6 and adjoining text)
KQX	dl	Shape constant for relationship between X:C and growth rate
S$_Q$	dl	Quotient for availability of limiting nutrient
X	mol L^{-1}	External concentration of nutrient X
XC	gX g^{-1}C	Ratio (quota) of X:C within phytoplankton
XC$_{min}$	gX g^{-1}C	Minimum quota of X:C
XC$_{max}$	gX g^{-1}C	Maximum quota of X:C
XCu	dl	Quotient describing the relationship between X:C and growth rate
XK$_g$	mol L^{-1}	Half-saturation concentration of nutrient X for growth when light is non-limiting
XK$_{gr}$	mol L^{-1}	Realized half-saturation concentration of nutrient X for growth
μ	gX g^{-1}X d^{-1}	X-specific growth rate
μ_{max}	gX g^{-1}X d^{-1}	Maximum X-specific growth rate

make initial comparisons in steady state. It is also worth noting that simulating the dynamics of photoacclimation requires more than just the inclusion of a dynamic mechanistic model but also a model structure that enables the adjustment of the rate of acclimation and, equally important, data against which to parameterize it (Flynn et al. 2001). There is thus an additional range of uncertainties inherent in the usage of the forward approach in non–steady-state conditions that I wished to avoid in this initial comparison.

Methods

Table 1 describes the parameters and units employed in the equations given below. Table 2 gives a summary overview of the models used in the simulations.

Construction of simple nutrient–PE relationships—In all models employed here, the form of the PE equation used is an exponential function (*see* eq. 6 in Jassby and Platt 1976, attributed to Webb et al. 1974). Technically, as respiration is not explicitly described in simple Monod-based models, references to PE curves are for net photosynthesis. All simulations performed for this work were run to steady state, where net photosynthesis equates to growth (i.e., PE equates to growth-E).

Typically (e.g., Evans and Garçon 1997), the inclusion of a nutrient interaction with the exponential PE curve descriptor, to give a nutrient–growth-E relationship, is given by Eq. 1.

$$\mu = S_Q\mu_{max}\left[1 - \exp\left(\frac{-\alpha^B E}{\mu_{max}}\right)\right] \qquad (1)$$

Here μ_{max} is the maximum growth rate, E irradiance, α^B the biomass-specific slope of the growth-irradiance curve, S_Q a

quotient describing the availability of the potentially limiting nutrient, and μ the resultant growth rate. The biomass units for α^B and μ_{max} are the same (typically in terms of C or N).

Outputs from the mechanistic models of N-photoacclimation described by Geider et al. (1998) and Flynn and Flynn (1998) are not best described by Eq. 1. Rather, the form of the nutrient–growth-E relationship, at least when S_Q is described in terms of just N, is described as in Eq. 2.

$$\mu = S_Q\mu_{max}\left[1 - \exp\left(\frac{-\alpha^B E}{S_Q\mu_{max}}\right)\right] \qquad (2)$$

In both instances, for a single limiting nutrient within a conventional Monod-type model, the quotient S_Q is described by a rectangular hyperbola (Michaelis–Menten equation). In a dual nutrient-limitation scenario, here for N and Fe, S_Q is given by Eq. 3, making use of a threshold control that assigns S_Q to the minimum of two hyperbolae.

$$S_Q = \min\left[\frac{N}{N + NK_g}, \frac{Fe}{Fe + FeK_g}\right] \qquad (3)$$

NK$_g$ and FeK$_g$ are half saturation constants defining the external nutrient concentration (N or Fe, respectively) at which, if no other factor is limiting, $\mu = \mu_{max}/2$.

There are two significant differences in the output of these nutrient-E formulations (Fig. 1). With Eqs. 2 and 3, the resultant nutrient-E interaction does not describe a decline of the initial slope of the total growth–irradiance relationship with increasing N-stress, only in the plateau. In turn, this has an important effect on nutrient limitation with increasing light limitation; the realized half saturation concentration of nutrient (K$_{gr}$) declines with growth at lower irradiance. Intuitively one may expect this to occur. However, with Eqs. 1 and 3, the value of K$_{gr}$ remains constant (and equal to K$_g$),

Table 2. Description of models described in the text.

Name	Description	Reference
GM	Single N-source–E mechanistic model with E-acclimation and forward computed Chl:C	Geider et al. 1998
MAP1	Full multi-nutrient (nitrate-ammonium-P-Si-Fe-E), internal-nutrient pools, mechanistic model with E-acclimation and forward computed Chl:C	Flynn 2001
MAP2	Simplified, quota-based, version of MAP1 with E-acclimation and forward computed Chl:C	Flynn 2003
MAP3	As MAP2 but with simple growth-E relationship and reverse computed Chl:C	Flynn 2003 + Eq. 2+3+8 (multi-nutrient)
MAP3c	As MAP3 but with modified FeC$_{min}$	Flynn 2003 + Eq. 2+3+9 (multi-nutrient)
Mono1	Monod-based model with N-E interaction and reverse computed Chl:C	Eq. 1+3+8 (single nutrient)
Mono2	Monod-based model with N-E interaction and reverse computed Chl:C	Eq. 2+3+8 (single nutrient)
Mono3	Monod-based model with N-Fe-E interaction and reverse computed Chl:C	Eq. 2+3+8 (multi nutrient)

while the effective value of α declines with poorer nutrient status (Fig. 1).

An argument for the use of Eq. 1 is that superficially, assuming Chl:N remains constant (as within the classic NPZ model—Fasham et al. 1990), the decline in α with poorer nutrient status is consistent with the results of Platt et al. (1992). However, in reality, Chl:N is not a constant, and the

Fig. 1. Implications of using alternative equations describing photosynthesis as a function of irradiance and nutrient availability. K_{gr} is the nutrient concentration required to support half maximal growth at a given irradiance; under light-saturating conditions, K_{gr} = K_g = 1 μmol L^{-1}. The lower panel shows effects on net growth (μ)—the uppermost curves in each series are for N-replete conditions, with the lowermost curves being most N-limiting.

field data of Platt et al. (1992) give photosynthesis rates and values of α^{Chl} from short-term PE incubations, not for growth-E. Although biologically speaking the use of Eq. 1 may be questioned (Flynn 2003), because this form is so widely used (Evans and Garçon 1997), both structures (Eqs. 1 and 2) were tested here.

The interaction between Fe and light limitations is more complex than that with N and light. This is because, assuming a fixed ratio of Fe to photosynthetic unit (PSU) and of Chl:PSU (Falkowski et al. 1981; Raven 1990), photoacclimation requires an increased Chl:C at lower irradiance and, hence, a pro rata increase in Fe:C. As a result, except at irradiance values so low that the organism is acclimated to contain the maximum Chl:C, K_{gr} for Fe increases with decreasing E (*see* Flynn 2003). This is in total contrast with the decline for NK_{gr} shown in Fig. 1 for a model using Eqs. 2 and 3. The greatest effect of Fe stress at low E, in the mechanistic N-Fe-E interaction model of Flynn and Hipkin (1999), is the limitation of the synthesis of Chl:C. However, at high E, more Fe is required to support nonphotosynthetic functions (respiration and, as applicable, nitrate reduction). The net result is that the values of α^C and the maximum photosynthetic rate both decline with Fe-stress. These interactions are described in Eq. 4; note that this equation describes interactions for a quota-based model, not a Monod model as employed with Eqs. 1 and 2.

$$\mu = \min[NCu, FeCu]\mu_{max}$$
$$\times \left[1 - \exp\left(-\alpha^C FeCu \frac{E}{\min[NCu, FeCu]\mu_{max}} \right) \right] \quad (4)$$

Here, NCu and FeCu are quotients (1 indicating no nutrient limitation and 0 maximum limitation) describing the relationship between the internal nutrient:C quota (for N and Fe, respectively) and growth rate, and α^C the C-specific initial slope of the PE curve. In comparison with Eq. 2, the only structural difference (other than the important linkage to internal nutrient quotas rather than external nutrient con-
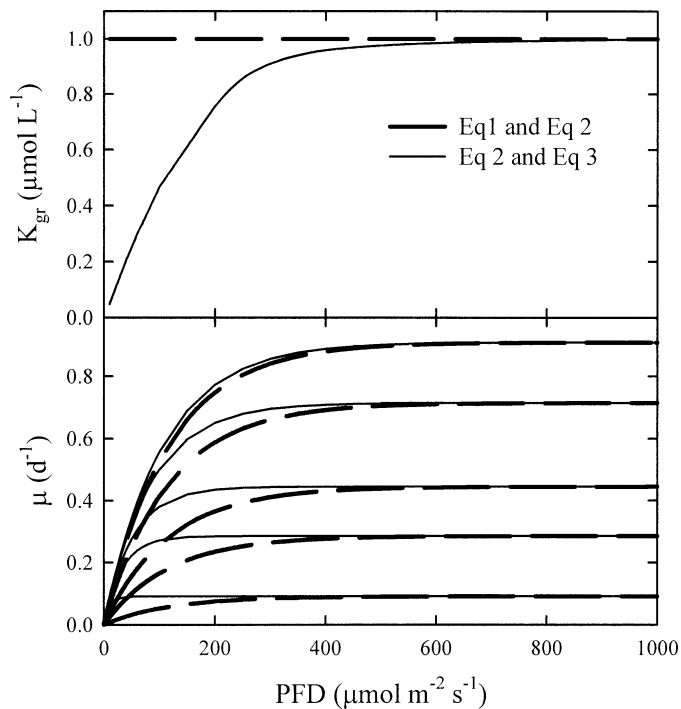
centrations) is that α^C is modified by the availability of Fe, as indexed to FeCu.

The form of the nutrient-status quotients used here is given in Eq. 5, relating the mass ratio X:C (where X is either N or Fe) to the minimum and maximum (XC_{min}, XC_{max}) quotas and to a dimensionless shape constant, KQX (for explanation and justification, *see* Flynn 2002a).

$$XCu = \frac{(1 + KQX)(XC - XC_{min})}{(XC - XC_{min} + KQX)(XC_{max} - XC_{min})} \quad (5)$$

A remaining point is that the minimum Fe quota (FeC_{min}), as used for the calculation of FeCu, is likely not a constant, but rather, one may expect it to increase with declining E in line with the higher Chl:C required to fix sufficient C at low E. Again, this is predicted in simulations run on the mechanistic model structure described by Flynn and Hipkin (1999), as shown in Flynn (2003). Equation 6 gives a correction for this event, where $FeCo_{min}$ and $FeCo_{max}$ are the minimum and maximum values, respectively, that FeC_{min} may take, and K_E a constant defining the shape of the light response curve. The value of K_E used here was 2.9 μmol photons m^{-2} s^{-1}, obtained from analysis of steady-state runs of the multinutrient mechanistic model MAP1 (Flynn 2001) at different irradiance values under Fe-limiting conditions.

$$FeC_{min} = FCo_{max} - \left[\frac{E}{E + K_E}(FeCo_{max} - FeCo_{min}) \right] \quad (6)$$

Derivation of Chl:C—Given the relationship between light, α^{Chl}, Chl:C, and gross growth rate when photosynthesis is not limited by Calvin cycle processes (Eq. 7), and supported by inspection of the output generated by the photoacclimative models of Flynn and Flynn (1998) and Geider et al. (1998), one may propose Eq. 8 to provide a simple description of Chl:C related to the output of Eqs. 1, 2, or 4.

$$\mu = ChlC \cdot E \cdot \alpha^{Chl} \quad (7)$$

$$ChlC = ChlC_{min} + \frac{\mu}{E \cdot \alpha^{Chl}} \quad (8)$$

The latter part of Eq. 8 thus back-calculates the Chl:C needed to attain a given growth rate with the supplied E and a set value of α^{Chl}. The addition of the minimum value of Chl:C ($ChlC_{min}$), which is the value of ChlC at very high E, gives an offset. As elsewhere in this work, photoinhibition is considered to be negligible.

Under Fe-stress one may expect the cell not to expend Fe on the construction of surplus PSUs and, hence, that the value of $ChlC_{min}$ would decline with Fe-stress. This is what the model of Flynn and Hipkin (1999) predicts. This is implemented within Eq. 9.

$$ChlC = ChlC_{min} \cdot FeCu + \frac{\mu}{E \cdot \alpha^{Chl}} \quad (9)$$

Models and scenarios—The aim of this work was to test whether a reverse calculation of Chl:C and nutrient-E growth limitation generated by simple models could match the output of mechanistic models. The chosen mechanistic models were the photoacclimative N-E model of Geider et al. (1998), hereafter GM, and the photoacclimative N-Fe-E Model of Algal Physiology, hereafter MAP2, described in Flynn (2003). MAP2 is a simplified form of the full N-P-Si-Fe-E model (MAP1) described earlier by Flynn (2001). A comparison between the photoacclimation approaches used in GM and within the MAP series of models showed similar outputs (Flynn et al. 2001). A modified form of GM was suggested by Flynn et al. (2001) to be the mechanistic model of choice if only a single N-source -E interaction is to be considered.

Models were built on Powersim Constructor with tuning (optimization) performed using Powersim Solver. Thus, GM and MAP2 were run to steady state at 10 different values of E (under constant illumination) with different levels of N-limitation (fixed external N concentration) and, in the case of MAP2, also with different levels of Fe-limitation. These simulations generated data series against which the simple reverse operating nonphotoacclimative models were tuned. Tuning for each simple model was thus performed simultaneously against the output of the source model run under different conditions, generating a common (and hence compromise) set of constants. These simple models were Monod-based, constructed from combinations of Eqs. 1, 2, 3, and 8 and an alternative, nonphotoacclimative version of MAP2 (i.e., MAP3) that employed combinations of Eqs. 4, 5, and 6 with Eqs. 8 or 9. Table 2 gives a summary of model descriptions, while Table 3 indicates the tunings and the resultant constants from those tuning processes.

Results and discussion

Tuning a N-E Monod model comprising Eqs. 1, 3, and 8 (Mono1) or Eqs. 2, 3, and 8 (Mono2) against GM over a range of N concentrations and irradiance values resulted in quite acceptable regressions both for μ and for Chl:C (Fig. 2, Table 4). The traditional growth-E equation (Eq. 1) used in Mono1 was slightly less satisfactory for both regressions than the interactive equation (Eq. 2) used in Mono2, but there appears to be no cause for concern in the widespread application of the biologically questionable Eq. 1 rather than Eq. 2. Moreover, there appears to be little justification for using the complex photoacclimative model GM rather than either of the Monod-based models, provided there is no requirement for matching the temporal dynamics of photoacclimation. It is not possible for such Monod-based models to reproduce these dynamics (as quota-based photoacclimative models can; Flynn et al. 2001), because growth is related directly to external conditions rather than to internal nutrient availability (and, hence, to cellular nutrient status). The Monod-based models can only be operated within a light–dark illumination cycle by making reference to day-averaged E and μ; typically the diurnal light cycle is not simulated explicitly in oceanographic models (*see* Flynn and Fasham 2003), so this is not a problem.

For consideration of the usefulness of a simple Monod-based N-Fe-E model, the N-E photoacclimative GM model used as the control was replaced with MAP2, a quota-based

Table 3. Model constants; see text for further information. Output from MAP2 operating with only N and/or E limitation was used to tune GM to establish a similar output between these two complex photoacclimative models (in bold). The simple models were then tuned against these outputs, as indicated. Units for α^{Chl} are μgC g^{-1}Chl μmol^{-1} photon m^{-2}; for α^{C} are μgC g^{-1}C μmol^{-1} photon m^{-2}. —, constants that were absent from that model structure; *, equates to constant Pcm defiend in Flynn et al. (2001); dl, dimensionless.

Model	Tuned against	μ_{max} (d^{-1})	α^{Chl}	α^{C}	ChlC$_{min}$ (gCh g^{-1} C)	NKg (μmol L^{-1})	KFe (nmol L^{-1})	KQFe (dl)
GM	**MAP2**	**1.483***	**2.05**	—	—	**0.50**	—	—
Mono1	GM	0.779	2.31	0.265	0.0111	0.14	—	—
Mono2	GM	0.858	2.30	0.198	0.0084	1.35	—	—
MAP2	**(control)**	**1.000**	**5.00**	—	—	**1.00**	**1.000**	—
Mono3	MAP2	0.792	2.56	0.134	0.0010	0.65	0.032	—
MAP3	MAP2	0.824	4.25	0.231	0.0026	1.00	1.000	0.030
MAP3c	MAP2	0.825	4.18	0.235	0.0025	1.00	1.000	0.061

photoacclimative model configured for multinutrient interactions (Table 2). The control model, now MAP2, was again run over a series of different conditions, and the test model (Mono3, using Eqs. 2, 3, and 8, with inclusion of a second nutrient [Fe]) was tuned to that output (Fig. 3, Table 3). Again, output was quite acceptable, returning growth rates and values of Chl:C in keeping with the output from the mechanistic model (Table 4).

From the above discussion, one may conclude that if the primary concern is the simulation of growth rates and Chl: C, then Monod-type models, as described above, can be quite adequate. However, it is more likely the case that the removal of nutrients from the water is also a required output in the simulation. A major problem with the Monod model
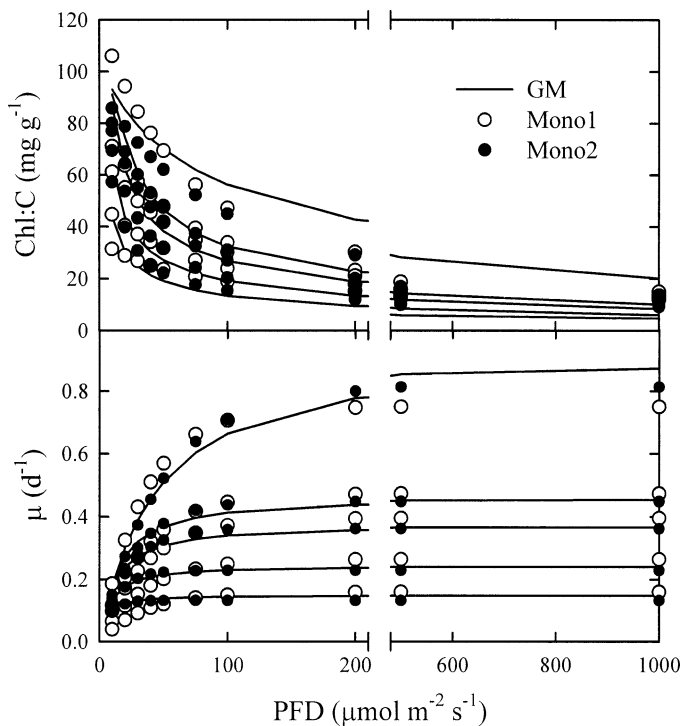

Fig. 2. Comparison of the steady-state output of model GM under N-E limitation, versus Mono1 (using Eq. 1) and Mono2 (using Eq. 2). The uppermost of the GM lines is for where N is replete, the lowermost for where N is most limiting. See also Tables 2 and 4.

(and the Shuter model; Shuter 1979) is that for multinutrient limitations, it displays various levels of dysfunctionality associated with the flawed assumption of fixed elemental ratios (C:N:P:Si:Fe) within the phytoplankton. Monod- or Shuter-based models should therefore not be used in multinutrient simulators (Flynn 2003). Suitably constructed quota-based models (Flynn 2003) are preferable for such applications, because they enable a proper simulation of variable cellular elemental ratios and, hence, of variable nutrient removal from the water.

So, turning now to the placement of reverse-derived Chl: C in quota-based models, comparisons were made between MAP2 and MAP3 (Fig. 3); these models are identical except for the description of Chl:C and the route by which Fe:C interacts with growth rate (Table 2). Not surprisingly (given the match between Mono3 and MAP2, and that MAP3 contained Chl:C components analogous to those in Mono3; Table 2), MAP3 gave a quite acceptable fit to the MAP2 output (Fig. 3, Table 4). There was a slight improvement in the simulation of Fe-limited growth when Eq. 6 was used to modify FeC$_{min}$ with E (model MAP3c; Tables 2, 4), but this is insufficient to justify the additional effort in the absence of experimental data to support the contention that FeC$_{min}$ does indeed vary with E (*see* text for Eq. 6). Again, operation of MAP3 within a light–dark cycle requires the use of day-averaged E and growth rates; otherwise, extreme oscillations occur in Chl:C and also in FeCu if Eq. 6 is used (MAP3c).

In general, all the short-cut, reverse calculation methods gave outputs that are very similar to those associated with the far more complex photoacclimation models when run under steady-state conditions (Table 4). Potential inadequacies arise only when one considers the fit of Chl:C values over the whole range of test conditions, in comparison with that predicted by the mechanistic models GM and MAP2 (Figs. 2, 3). However, one may question how important this is, given the lack of strong data for the real relationship of Chl:C and nutrient interactions for a wide range of phytoplankton species. The data tabulated in MacIntyre et al. (2002) show that there are remarkably few data for Chl-specific α (α^{Chl}) and for Chl:C$_{max}$, required to parameterize forward-computing models, and many of these data are not available for ecologically important marine species. Unless we assume that these values are truly representative of field

Table 4. Regression analysis for the comparisons shown in Figs. 2 and 3. An optimal fit would give a slope and r² of 1. n = 50 for each GM regression, and n = 90 for each MAP2 regression.

		(Fig. 2) GM versus:		(Fig. 3) MAP2 versus:		
		Mono1	Mono2	MAP3	MAP3c	Mono3
μ	slope	0.982	0.993	0.967	0.969	0.983
	r^2	0.947	0.988	0.951	0.955	0.940
Chl:C	slope	0.953	0.962	0.957	0.962	0.914
	r^2	0.891	0.934	0.925	0.936	0.833

organisms, we may be introducing no greater a degree of error using a reverse approach for a description of a generic phytoplankton population.

Any model can only be as good as its weakest component; in oceanographic models, there is considerable uncertainty over the light field within the mixed layer depth and indeed over the merits of using Eulerian-continuum or Lagrangian-ensemble approaches for the description of phytoplankton within the vertical water structure (Woods and Onken 1982; Barkmann and Woods 1996; Flynn and Fasham 2003). Differences in the physiology of the phytoplankton are also given scant regard, perhaps being limited to division into groups, such as diatoms and nondiatoms, for example, which themselves encompass a very wide range of ecophysiological capabilities. Given all these issues, output differences between forward and reverse methods for deriving growth rates and Chl:C may arguably become increasingly minor, if not irrelevant, for many simulation scenarios.

However, there are instances in which the differences between the modeling approaches are likely to be important. These hinge around the rate of photoacclimation and around factors such as the response rate to Fe-refeeding. The reverse

calculation of Chl:C gives an instantaneous response that is not only incorrect, it also leads to computational problems in darkness (*see* discussion in Flynn et al. 2001). These may be of particular significance for scenarios such as the dynamics of bloom development, simulations of vertically migrating algae, whose changes in Chl:C with photoacclimation affect the growth of other algae through shading (Flynn and Fasham 2002; Flynn 2002*b*), and with Fe fertilization. However, even here, the use of quota-based models rather than Monod-based models will inevitably introduce a measure of temporal dynamics in acclimation responses even where an instantaneous reverse method is used to derive Chl:C. Also, as noted at the beginning of this article, the use of forward methods in non–steady-state conditions requires an adequate tuning of the rate of acclimation, a feature that was not supported in the original model of Geider et al. (1998), as discussed in Flynn et al. (2001).

To conclude, there appears to be little justification within simple models of phytoplankton growth, as used in most oceanographic simulators, to employ a mechanistic photoacclimative approach. Even in multinutrient scenarios, unless there is a specific requirement to simulate the temporal dynamics of photoacclimation, including simulations of Fe-refeeding, then a reverse calculation approach seems quite acceptable. This is especially the case given that Monod, Shuter, and simple quota models should be avoided in such scenarios (Flynn 2003). One could thus argue that the selection of forward rather than reverse methods to describe Chl:C is the least of our concerns in the derivation of multinutrient models; it is more important to get the underlying basis of the model correct.
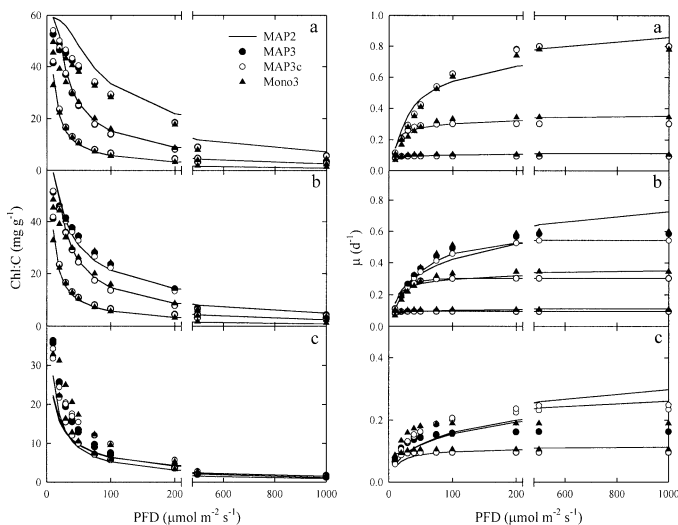

Fig. 3. Comparison of the steady-state output of model MAP2 under N-Fe-E limitation, versus MAP3 (not accounting for changes in FeC$_{min}$), MAP3c (accounting for changes in FeC$_{min}$), and Mono3 (same as Mono2, but including Fe-stress interaction). In each panel, the uppermost data set is N-replete and the lowermost N-limiting. Panels a are Fe-replete, and panels c are most Fe-limiting. Some combinations of N-Fe-E limitation give similar μ or Chl:C. See also Tables 2 and 4.

References

BARKMANN, W., AND J. D. WOODS. 1996. On using a Lagrangian model to calibrate primary production determined from in vitro incubation measurements. J. Plankton Res. **18:** 767–788.

BEHRENFELD, M. J., E. MARAÑÓN, D. A. SIEGEL, AND S. B. HOOKER. 2002. Photoacclimation and nutrient-based model of light-saturated photosynthesis for quantifying oceanic primary production. Mar. Ecol. Prog. Ser. **228:** 103–117.

CLOERN, J. E., C. GRENZ, AND L. VIDERGAR-LUCAS. 1995. An empirical model of the phytoplankton chlorophyll:carbon ratio—the conversion factor between productivity and growth rate. Limnol. Oceanogr. **40:** 1313–1321.

DONEY, S. C., D. M. GLOVER, AND R. G. NAJJAR. 1996. A new coupled, one-dimensional biological-physical model for the upper ocean: Application to the JGOFS Bermuda Atlantic Time Series Study (BATS) site. Deep-Sea Res. II **43:** 591–624.

EVANS, G. T., AND V. C. GARÇON [Eds.]. 1997. One-dimensional

models of water column chemistry. JGOFS Report 23/97. JGOFS Bergen, Norway.

FALKOWSKI, P. G., T. G. OWENS, A. C. LEY, AND D. C. MAUZERALL. 1981. Effect of growth irradiance levels on the ratio of reaction centers in 2 species of marine phytoplankton. Plant Physiol. **69:** 969-973.

FASHAM, M. J. R., H. W. DUCKLOW, AND S. M. MCKELVIE. 1990. A nitrogen-based model of plankton dynamics in the oceanic mixed layer. J. Mar. Res. **48:** 591–639.

FLYNN, K. J. 2001. A mechanistic model for describing dynamic multi-nutrient, light, temperature interactions in phytoplankton. J. Plankton Res. **23:** 977–997.

———. 2002*a*. How critical is the critical N : P ratio? J. Phycol. **38:** 961–970.

———. 2002*b*. Toxin production in migrating dinoflagellates: A modelling study of PSP producing *Alexandrium.* Harmful Algae **1:** 147–155.

———. 2003. Modelling multi-nutrient interactions in phytoplankton; Balancing simplicity and realism. Prog. Oceanogr. **56:** 249–279.

———, AND M. J. R. FASHAM. 2002. A modelling exploration of vertical migration by phytoplankton. J. Theor. Biol. **218:** 471–484.

———, AND ———. 2003. Operation of light–dark cycles within simple ecosystem models of primary production and the consequences of using phytoplankton models with different abilities to assimilate N in darkness. J. Plankton Res. **25:** 83–92.

———, AND K. FLYNN. 1998. The release of nitrite by marine dinoflagellates—development of a mathematical simulation. Mar. Biol. **130:** 455–470.

———, AND C. R. HIPKIN. 1999. Interactions between iron, light, ammonium and nitrate; Insights from the construction of a dynamic model of algal physiology. J. Phycol. **35:** 1171–1190.

———, H. MARSHALL, AND R. J. GEIDER. 2001. A comparison of two N-irradiance models of phytoplankton growth. Limnol. Oceanogr. **46:** 1794–1802.

GEIDER, R. J., H. L. MACINTYRE, AND T. M. KANA. 1998. A dynamic regulatory model of phytoplankton acclimation to light, nutrients and temperature. Limnol. Oceanogr. **43:** 679–694.

HURTT, G. C., AND R. A. ARMSTRONG. 1996. A pelagic ecosystem model calibrated with BATS data. Deep-Sea Res. II **43:** 653–683.

JASSBY, A. D., AND T. PLATT. 1976. Mathematical formulation of the relationship between photosynthesis and light for phytoplankton. Limnol. Oceanogr. **21:** 540–547.

KIEFER, D. A., AND B. G. MITCHELL. 1983. A simple, steady-state description of phytoplankton growth based on absorption cross section and quantum efficiency. Limnol. Oceanogr. **28:** 770–776.

LAWS, E. A., AND T. T. BANNISTER. 1980. Nutrient- and light-limited growth of *Thalassiosira fluviatilis* in continuous culture, with implications for phytoplankton growth in the ocean. Limnol. Oceanogr. **25:** 457–473.

———, AND M. S. CHALUP. 1990. A microalgal growth model. Limnol. Oceanogr. **35:** 597–608.

MACINTYRE, H. L., T. M. KANA, T. ANNING, AND R. J. GEIDER. 2002. Photoacclimation of photosynthesis irradiance response curves and photosynthetic pigments in microalgae and cyanobacteria. J. Phycol. **38:** 17–38.

MARAÑÓN, E., AND P. M. HOLLIGAN. 1999. Photosynthetic parameters of phytoplankton from 50°N to 50°S in the Atlantic Ocean. Mar. Ecol. Prog. Ser. **176:** 191–203.

PLATT, T., S. SATHYENDRANATH, O. ULLOA, W. G. HARRISON, N. HOEPFFNER, AND J. GOES. 1992. Nutrient control of phytoplankton in the Western North Atlantic. Nature **356:** 229–231.

RAVEN, J. A. 1990. Predictions of Mn and Fe use efficiencies of phototrophic growth as a function of light availability for growth and of C assimilation pathway. New Phytol. **116:** 1–18.

SHUTER, B. 1979. A model of physiological adaptation in unicellular algae. J. Theor. Biol. **78:** 519–552.

WEBB, W. L., M. NEWTON, AND D. STARR. 1974. Carbon dioxide exchange of *Alnus rubra*: A mathematical model. Oecologia **17:** 281–291.

WOODS, J. D., AND R. ONKEN. 1982. Diurnal variation and primary production in the ocean—preliminary results of a Lagrangian Ensemble method. J. Plankton Res. **4:** 735–756.

ZONNEVELD, C. 1998. A cell-based model for the chlorophyll *a* to carbon ratio in phytoplankton. Ecol. Model. **113:** 55–70.